

Effects of nonmagnetic scatterers on the local density of states around a vortex in *s*-wave superconductors

P. Miranović

Department of Physics, University of Montenegro, 81000 Podgorica, Serbia and Montenegro

M. Ichioka and K. Machida

Department of Physics, Okayama University, 700-8530 Okayama, Japan

(Received 17 December 2003; revised manuscript received 13 April 2004; published 20 September 2004)

We study the effect of nonmagnetic impurities on the local density of states (LDOS) in the mixed state of *s*-wave superconductors. The quasiclassical equations of superconductivity in the vortex state are solved self-consistently to show how the LDOS evolves with impurity concentration. The spatially averaged zero-energy LDOS is a linear function of magnetic induction in low fields, $N(E=0) = \alpha(\tau)B/H_{c2}$, for all impurity concentrations. The coefficient α depends weakly on the electron mean-free path. We evaluate numerically the differential conductance and spatial profiles of zero-energy LDOS, which can help in extracting the mean-free path from the measured LDOS.

DOI: 10.1103/PhysRevB.70.104510

PACS number(s): 74.25.Jb, 74.25.Bt, 74.25.Op

I. INTRODUCTION

Since Hess and co-workers¹ succeeded in measuring the local density of states (LDOS) in the superconducting NbSe₂, there have been many reports and theoretical studies on the electronic structure of superconductors in the mixed state. The experimental technique, the scanning tunneling spectroscopy, enables one to measure the differential conductivity $\sigma(\mathbf{r}, V)$ as a function of positions \mathbf{r} and bias voltages V . $\sigma(\mathbf{r}, V)$ is closely related to the LDOS $N(\mathbf{r}, E)$

$$\frac{\sigma(\mathbf{r}, V)}{\sigma_N} = \int_{-\infty}^{\infty} \frac{dE}{4TN_0} \frac{N(\mathbf{r}, E) \cosh^2((E + eV)/2T)}{\cosh^2((E + eV)/2T)}, \quad (1)$$

where σ_N is the normal state differential conductivity, e is electron charge, E is the energy relative to the Fermi level, and N_0 is DOS at the Fermi level in the normal state; $k_B = 1$. At zero temperature, $\sigma(\mathbf{r}, V)$ and LDOS are proportional: $\sigma(\mathbf{r}, V)/\sigma_N = N(\mathbf{r}, |e|V)/N_0$. This is not the case for $T \neq 0$; in general, the $\sigma(\mathbf{r}, V)$ can be considered as a thermally broadened LDOS.

At low temperatures, $\sigma(\mathbf{r}, V)$ should follow the spatial structure of the LDOS. Two prominent features should be mentioned. $\sigma(\mathbf{r}, V)$ measured at the vortex center of high-quality NbSe₂ crystals revealed a peak at the Fermi level (the zero-bias peak) that well exceeds σ_N .¹ This indicates that vortex core can not be viewed as being “normal,” at least in clean superconductors. The zero-bias peak in $\sigma(\mathbf{r})$ originates from the zero energy peak of LDOS at the vortex center, which is due to the low lying bound states inside the vortex core. The other remarkable feature revealed in Ref. 1 is a star-shaped $\sigma(\mathbf{r})$ around the vortex core measured at a fixed voltage, with the star orientation depending on the voltage bias. The sixfold structure of $\sigma(\mathbf{r})$ in NbSe₂ may come from the effect of the hexagonal vortex lattice, or may be caused either by the anisotropic *s*-wave pairing or by the anisotropic Fermi surface. Whatever the dominant effect is, the star-

shaped $\sigma(\mathbf{r})$ correlates with the star-shaped LDOS of the vortex lattice.

Still, the measured $\sigma(\mathbf{r}, V)$ does not follow the sharp features of the theoretically calculated LDOS even when the experiment is done at very low temperatures.² The height and width of the zero-bias peak are found to be sample dependent, indicating the effect of impurities as a plausible explanation. This calls for a quantitative study of the effect of impurities upon the LDOS, the purpose of our paper.

Also, we consider the effect of impurities on the field dependence of specific heat. In *s*-wave superconductors, low-energy quasiparticles are trapped in vortex cores. As a result, the spatially averaged zero-energy LDOS is proportional to the density of vortices: $N(E=0) \propto N_0 \xi^2 B$ (B is the magnetic induction, ξ is the vortex core size). This translates to the linear field dependence of the low-temperature specific heat given by $C_s/T = 2\pi^2 N(E=0)/3$. The nonlinearity in the low field $C_s(B)$ should be related to the gap anisotropy. In the case of anisotropic *s*-wave pairing, nonmagnetic impurities smear out the gap anisotropy; this affects $C_s(B)$ curves. This kind of experiment has been performed on Nb_{1-x}Ta_xSe₂ (Ref. 3) and Y(Ni_{1-x}Pt_x)₂B₂C with the intention to make the gap isotropic by adding impurities.^{3,4} Thus, it is of interest to study how the field dependence of spatially averaged LDOS evolves with impurity concentration, starting with *s*-wave superconductors.

So far, the only systematic experimental study of the effect of disorder on LDOS is by Renner *et al.*⁵ In particular, they measured the zero-bias $\sigma(\mathbf{r})$ at the vortex center in the alloy Nb_{1-x}Ta_xSe₂. The Ta substitution of Nb leads to a systematic decrease of the electron mean-free path, whereas the electronic spectrum is expected to change little, since Nb and Ta are isoelectronic and have close atomic radii. The zero-energy $\sigma(\mathbf{r})$ is found to be very sensitive to the impurity concentration. It gradually disappears, and for $x=0.2$, the zero-energy LDOS at the vortex center is the same as that of the normal phase N_0 . It was even proposed that $\sigma(\mathbf{r}, V)$ spectra can serve as a measure of quasiparticle scattering time.

In this paper, the problem of LDOS in the presence of nonmagnetic impurities is studied with the help of the quasiclassical equations of superconductivity. This approach (adequate when the coherence length ξ is much larger than the atomic scale k_F^{-1}) has been used by Ullah *et al.*⁶ and Klein⁷ to study LDOS for an isolated vortex in clean isotropic s -wave materials with only qualitative estimates of impurity effects. The full self-consistent analysis of LDOS in a vortex lattice has been performed by Ichioka *et al.* in superconductors without impurities.⁸ In Refs. 9 and 10 the effect of impurities was studied for single vortices. The effect of impurities on DOS in extremely high fields, where the Landau level quantization of the electronic energies should be taken into account, has been studied by Dukan and Tešanović;¹¹ these phenomena are beyond the scope of this text. Also, for the extreme dirty case, the reader is referred to Refs. 12 and 13. In this work, we calculate LDOS in the vortex lattice by systematically changing the impurity concentration, and analyze the field dependence of the spatially averaged zero-energy LDOS and the core radius. These are done for the isotropic s -wave case, which needs to be clarified before the additional effect of gap anisotropy is included.

The paper is organized as follows. In Sec. II, the method of solving Eilenberger equations is described (a reader not interested in technical details may skip this section). In Sec. III, the spatial and energy dependencies of the LDOS and $\sigma(\mathbf{r}, V)$ for various impurity concentrations are given. In Sec. IV, the effect of impurities on the specific-heat field dependence is discussed.

II. METHOD

One of the difficulties in the numerical solving of the Eilenberger equations for the mixed state is in posing the boundary conditions. One way to overcome this is to use a special gauge in which the Green's functions are periodic, and to work in Fourier space (periodic boundary condition).¹⁴ Another method is based on the fact that during the integration process, the Green's functions grow exponentially (explode). Fortunately, unphysical solutions can be manipulated to form the physical ones; this is the essence of the so-called "explosion method."^{8,15,16} We use an approach based on transforming Eilenberger equations to the Riccati form.^{18,19} The method has a clear advantage of avoiding unphysical solutions altogether, and the solutions generated are numerically stable.

For an s -wave superconductor in the presence of nonmagnetic impurities, the equations for the Eilenberger Green's functions f , f^\dagger , and g are

$$[\omega + \mathbf{u} \cdot (\nabla + i\mathbf{A})]f = \Psi g + Fg - Gf, \quad (2)$$

$$[\omega - \mathbf{u} \cdot (\nabla - i\mathbf{A})]f^\dagger = \Psi^* g + F^* g - Gf^\dagger. \quad (3)$$

Here, $\omega = t(2n+1)$ is Matsubara frequency with an integer n , \mathbf{u} is unit vector of the Fermi velocity, and the impurity potentials

$$F = \frac{1}{\tau} \langle f \rangle, \quad G = \frac{1}{\tau} \langle g \rangle. \quad (4)$$

The Fermi surface is assumed to be isotropic and two dimensional (2D).¹⁷ Averages over the isotropic cylindrical Fermi surface reduce to $\langle \dots \rangle = (1/2\pi) \int \dots d\varphi$, the average over the polar angle φ .

Equations (2) and (3) are supplemented by the self-consistency equations for the gap function Ψ and the vector potential \mathbf{A}

$$\Psi \ln t = 2t \sum_{\omega>0} \left[\langle f \rangle - \frac{\Psi}{\omega} \right], \quad (5)$$

$$\nabla \times \nabla \times \mathbf{A} = -\frac{2t}{\tilde{\kappa}^2} \text{Im} \sum_{\omega>0} \langle ug \rangle, \quad (6)$$

where $t = T/T_c$ is the reduced temperature.

The Born approximation is assumed in treating scattering on impurity. For convenience, equations are written in dimensionless units: the order parameter Ψ is measured in units πT_c ; $R_0 = v/(2\pi T_c)$ is taken as a unit of length, where v is Fermi velocity; the magnetic field is in units $H_0 = \Phi_0/2\pi R_0^2$, where Φ_0 is flux quantum. Furthermore, the vector potential is in units $A_0 = \Phi_0/2\pi R_0$, the energy in units $E_0 = (\pi T_c)^2 N_0 R_0^3$, and the scattering time τ is in units $l/(2\pi T_c) = l/0.882\xi_0$, with the electron mean-free path l and ξ_0 being the BCS coherence length.

The Eilenberger parameter $\tilde{\kappa}$ is the only material constant that enters the equations

$$\tilde{\kappa}^2 = 2\pi N_0 \left(\frac{\pi}{\Phi_0} \right)^2 \frac{v^4}{(\pi T_c)^2}. \quad (7)$$

It is related to Ginzburg-Landau (GL) parameter κ via $\tilde{\kappa}^2 = [7\zeta(3)/18]\kappa^2$ in the three dimensional (3D) case and

$$\tilde{\kappa}^2 = \frac{7\zeta(3)}{8} \kappa^2. \quad (8)$$

in the 2D case. Here ζ is Riemann's zeta function. Eilenberger Green's functions f , f^\dagger , and g are normalized so that $g = \sqrt{1 - ff^\dagger}$.

The quantity of our interest, the LDOS as a function of position \mathbf{r} and quasiparticle energy E , is defined as

$$N(\mathbf{r}, E) = N_0 (\text{Re } g(\mathbf{r}, \mathbf{u}, \omega \rightarrow \delta - iE)), \quad (9)$$

where the function g describes normal excitations and δ is a small number taking account of broadening levels. Following Schopohl, we introduce auxiliary functions a and b as follows:^{18,19}

$$f = \frac{2a}{1+ab}, \quad f^\dagger = \frac{2b}{1+ab}, \quad g = \frac{1-ab}{1+ab}. \quad (10)$$

The functions a and b satisfy the system of *decoupled* Riccati's differential equation

$$\mathbf{u} \cdot \nabla a = -(\omega + G + i\mathbf{u} \cdot \mathbf{A})a + \frac{\Psi + F}{2} - \frac{a^2}{2} (\Psi^* + F^*), \quad (11)$$

$$\mathbf{u} \cdot \nabla b = (\omega + G + i\mathbf{u} \cdot \mathbf{A})b - \frac{\Psi^* + F^*}{2} + \frac{b^2}{2}(\Psi + F). \quad (12)$$

Moreover, $a(\mathbf{r}, \mathbf{u}, \omega)$ and $b(\mathbf{r}, \mathbf{u}, \omega)$ are not independent. Once we solve the Eq. (11) for a , the function b can be readily calculated:

$$b(\mathbf{r}, \mathbf{u}, \omega) = -a^*(-\mathbf{r}, \mathbf{u}, \omega). \quad (13)$$

It is convenient for our purpose to work in local coordinates (ρ, η) at the Fermi cylinder, such that the Fermi velocity direction \mathbf{u} coincides with the ρ axis

$$\begin{aligned} \rho &= x \cos \phi + y \sin \phi, \\ \eta &= y \cos \phi - x \sin \phi. \end{aligned} \quad (14)$$

Then, Eq. (11) reduces to

$$\frac{\partial a}{\partial \rho} = -(\omega + G + i\mathbf{u} \cdot \mathbf{A})a + \frac{\Psi'}{2} - \frac{a^2 \Psi'^*}{2}, \quad (15)$$

where $\Psi' = \Psi + F$. Unlike the integration of Eilenberg equations, as given in Eqs. (2) and (3), where an exponentially growing (and thus, unphysical) solution dominates, in transformed Eqs. (11) and (12), we have the opposite tendency. Integrating Eq. (11) along the direction ρ to a desired point ρ' , the numerically stable solution a_+ is obtained. Note that integrating in the opposite direction, toward decreasing ρ , one gets a solution $a_- = -1/a_+$. The initial point in the integration process $\rho - \rho_{min}$ should be taken far from the point ρ' , which we want to calculate Eilenberger functions. To optimize the numerical calculation, one should always take the minimum integration path ρ_{min} , along which the numerical solution is stabilized. The integration path ρ_{min} value depends on the Matsubara frequency ω (real or complex) and on the impurity concentration.

We choose the gauge $\nabla \cdot \mathbf{A} = 0$ and separate the variable part of the vector potential \mathbf{A}' by writing

$$\mathbf{A}(\mathbf{r}) = \frac{\mathbf{B} \times \mathbf{r}}{2} + \mathbf{A}'(\mathbf{r}), \quad (16)$$

where \mathbf{B} is the magnetic induction, and $\mathbf{A}'(\mathbf{r})$ has the periodicity of the vortex lattice. Then, Eq. (6) takes the form

$$\nabla^2 \mathbf{A}' = \frac{2t}{\kappa^2} \text{Im} \sum_{\omega > 0} \langle u g \rangle. \quad (17)$$

This equation is linear in \mathbf{A}' and g , and easy to deal with in Fourier space.

The equilibrium vortex lattice is assumed hexagonal. It suffices to solve Eq. (15) in a primitive lattice cell; moreover, we can consider only velocity directions $0 < \varphi < \pi/6$. With the help of symmetry properties of $a(\mathbf{r}, \mathbf{u}, \omega)$ (which are the same as those of f , see Ref. 8), we can obtain a for all velocity directions.

Iteration procedure

As a starting ansatz we take the Abrikosov solution for $\Psi(\mathbf{r}), \mathbf{A}'(\mathbf{r}) = 0$, with the impurity potentials in the form

$$F = \frac{1}{\tau} \frac{\Psi(\mathbf{r})}{\sqrt{\omega^2 + |\Psi(\mathbf{r})|^2}}, \quad G = \frac{1}{\tau} \frac{\omega}{\sqrt{\omega^2 + |\Psi(\mathbf{r})|^2}}. \quad (18)$$

After solving Eq. (15), the new potentials are obtained from the self-consistency Eqs. (5), (6), and (4). The results are plugged back to the Eq. (15), which is solved again. This iterative procedure is repeated until the self-consistency is achieved. The maximum frequency $\omega_{cut} = t(2N_{cut} + 1)$ should be chosen so that the result does not depend on the choice of ω_{cut} . On the other hand, the number of iteration cycles needed to stabilize the pair potential increases with the N_{cut} . We followed Klein¹⁵ and choose $\omega_{cut} = 20\pi T_c$ (in common units) as appropriate for all temperatures. This gives $N_{cut} \sim \text{Int}(10/t)$. Fortunately, we do not have to solve (15) for all ω 's. For high frequencies, the solution can be well approximated by

$$a \approx \frac{1}{2} \left(\frac{1}{\omega'} - \frac{\mathbf{u} \cdot \mathbf{\Pi}}{\omega'^2} + \frac{(\mathbf{u} \cdot \mathbf{\Pi})^2}{\omega'^3} \right) (\Psi + F), \quad (19)$$

where $\omega' = \omega + 1/\tau$ and $\mathbf{\Pi} = \nabla + i\mathbf{A}$. We use Eq. (19) for $n > N_{cut}/2$.

The solution we look for is quasiperiodic: translations by $\mathbf{R}_{nm} = n\mathbf{r}_1 + m\mathbf{r}_2$ ($\mathbf{r}_1, \mathbf{r}_2$ are primitive cell vectors, n, m are integers) amount to a phase factor

$$a(\mathbf{r} + \mathbf{R}_{nm}, \mathbf{v}, \omega) = a(\mathbf{r}, \mathbf{v}, \omega) e^{i\chi(\mathbf{r}, \mathbf{R}_{nm})}, \quad (20)$$

where

$$\chi = \pi \left[\frac{mx}{a_0} - \frac{y(n + m \cos \beta)}{a_0 \sin \beta} + nm + n - m \right], \quad (21)$$

and $\beta = \pi/3$ is the angle between primitive vectors.

Once $\Psi(\mathbf{r}), \mathbf{A}(\mathbf{r})$, and $F(\mathbf{r}, \omega), G(\mathbf{r}, \omega)$ are calculated, the Eilenberger equations are solved again, but this time for $\omega = \delta - iE$. It has been noted^{20,21} that the density of states $N(E = 0)$ is sensitive to the value of δ . The point is that δ has roughly the same effect as impurities in suppressing the peak in the DOS at the vortex center. For small values of δ , $N(\mathbf{r}, E = 0)$ has sharp maxima at the vortex centers, and a fine mesh is needed to evaluate LDOS and their spatial averages. We find a negligible difference in LDOS (spatially averaged) for $\delta = 0.01$ and 0.001 . Thus, the parameter $\delta = 0.001$ suffices for our calculation, to avoid an additional broadening effect due to δ in spatially averaged LDOS.

III. LOCAL DENSITY OF STATES AND DIFFERENTIAL CONDUCTANCE

Properties of the vortex core are governed by Andreev bound states in the clean limit, while in the dirty case they are governed by normal electrons.²² The Andreev scattering from the pair potential (the order parameter) inside the core turns the electronlike excitations into holelike, and vice versa. At certain energies, the coherent superposition of particle and hole states is constructive, and bound states are formed. The energy of the lowest bound state is $E \sim \Delta/k_F \xi$. In the quasiclassical limit $k_F \xi \gg 1$, the lowest bound state energy is pushed to zero. The zero-energy bound state in the core manifests itself as a peak in zero-energy LDOS at the

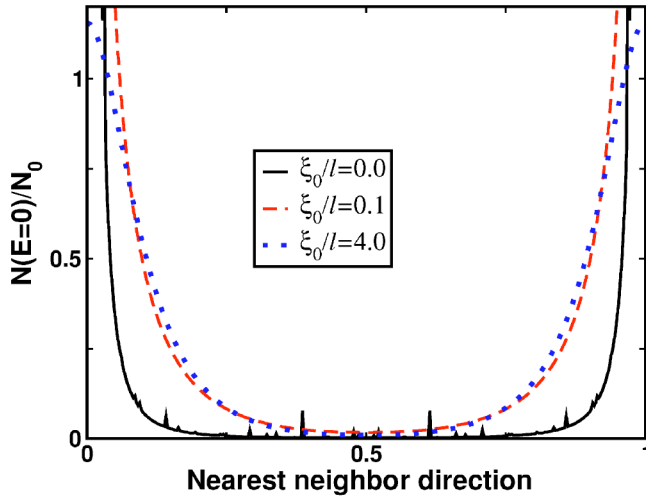


FIG. 1. The spatial variation of zero-energy DOS along the nearest-neighbor direction. The solid line corresponds to the clean limit; dashed lines are calculated for $\xi_0/\ell=0.1$ and $\xi_0/\ell=4.0$. The calculation is performed at approximately the same relative field, $B=0.1H_{c2}$.

vortex center. Scattering on impurities randomizes the quasiparticle motion, and they lose information on their initial state. Thus, the impurities smear out the sharp structure of LDOS. To illustrate this, we focus on the spatial structure of zero-energy LDOS $N(\mathbf{r}, E=0)$.

In Fig. 1, the spatial variation of the LDOS along the line connecting two nearest-neighbor vortices is shown. Data for a clean superconductor, $\xi_0/\ell=0.0$, for a relatively large mean-free path, $\xi_0/\ell=0.1$, and for an impure case $\xi_0/\ell=4.0$, are presented. The points 0 and 1 on the horizontal axis are the position of vortex centers.

To remind the reader again, in the clean limit, the height and width of the LDOS peak depend on the small parameter δ , which measures how far we are from the pole of the Green function g . In this sense, the height and width of the peak in the clean limit are arbitrary. However, spatial integration of this LDOS peak is almost independent of the parameter δ , if we use sufficiently small δ .

At the vortex center, zero-energy DOS, $N(E=0, \mathbf{r}=0)$ in the clean limit, greatly exceeds the normal state value N_0 . When this was originally observed,¹ it looked at odds with the generally accepted naive picture of the vortex core as being “normal.” Analyzing the zero- E DOS, $N(0, \mathbf{r})$ in the impure case, we see that the purity of the sample is crucial in forming the main peak at the vortex center. In the dirty limit ($\xi_0/\ell \rightarrow \infty$), $N(0, \mathbf{r})$ within the vortex core approaches the normal state value N_0 , and only in this limit can one view the vortex core as being “normal.” Even a weak impurity scattering has a strong impact on the $N(0, \mathbf{r})$ profile.

To understand the LDOS behavior in more detail, we also consider the profile of the order parameter $|\Psi(\mathbf{r})|$, and define the core radius ξ by $1/\xi = (\partial|\Psi(\mathbf{r})|/\partial r)_{r=0}/|\Psi_{NN}|$, where $|\Psi_{NN}|$ is the maximum value of the order parameter along the nearest-neighbor direction, and a derivative is taken along the same direction. A comparison of the ideal case of a clean superconductor $\xi_0/\ell=0$, with the rather pure case of ξ_0/ℓ

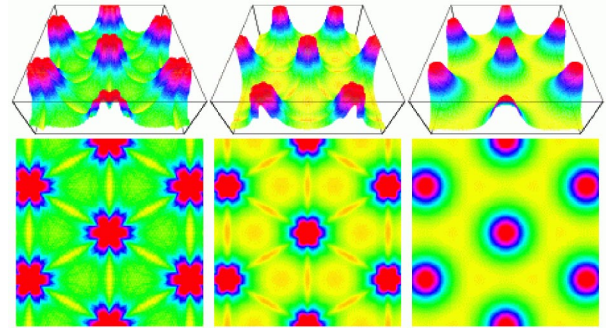


FIG. 2. The zero-energy DOS within the vortex lattice for superconductors with $\xi_0/\ell=0.0, 0.1$, and 4.0 (in order from left to right). Only data points $N(E=0)/N_0 < 1$ are presented. The small parameter $\delta=0.03$ is used for clean limit data to clarify the spatial distribution.

$=0.1$, reveals a change of the vortex core size by a factor of 2. It should be noted that $N(0, \mathbf{r})$ averaged over the lattice cell is approximately the same in all cases: an increase of the core size is accompanied by a reduction of the peak height.

It is instructive to see how the spatial structure of the zero-energy DOS $N(0, \mathbf{r})$ within the vortex lattice evolves when impurities are added. In the clean limit, $N(0, \mathbf{r})$ around the single vortex is cylindrically symmetric. As soon as the vortex lattice is formed, the cylindrically symmetric $N(0, \mathbf{r})$ gives way to a star-shaped structure within the hexagonal lattice.⁸ This is seen in Fig. 2. The effect of the vortex lattice notwithstanding, the other factors, such as anisotropies of the pairing function²³ and of the Fermi surface, can also contribute to the details of the star-shaped structure. By reducing the mean-free path, the star-shaped modulation of $N(0, \mathbf{r})$ gradually disappears and is completely absent in the dirty limit, even at relatively high fields. Thus, the periodicity of the order parameter is not the only element determining the structure of $N(0, \mathbf{r})$ in Fig. 2. Only in pure s -wave superconductors do the coherent superposition of electron and hole states in the periodic lattice account for the star-shaped $N(0, \mathbf{r})$.

In Fig. 3(a), the LDOS at the vortex center is plotted as a function of quasiparticle excitation energy E (in units of πT_c) for the clean case. The LDOS oscillates with energy, the result previously reported in Ref. 24. This phenomenon has the same origin as oscillations of DOS in superconducting-normal proximity systems:^{25,26,28} the interference of quasiparticles reflected at the superconducting-normal interface. The mixed state can be viewed as periodically arranged “normal”-superconducting boundaries. In Fig. 3(b), we show the differential conductivity at $T=0.1T_c$ calculated according to Eq. (1). It is seen that at this temperature, $\sigma(E)$ is the thermally broadened LDOS, but the oscillating pattern is still visible.

In Fig. 4, the LDOS at the vortex center as a function of energy is plotted for a few values of the mean-free path ℓ . The amplitude of oscillations is sensitive to impurities and is nearly lost even in clean samples with $\xi_0/\ell=0.1$. Proliferating impurities cause a flattening of the LDOS at the vortex center: the zero-energy peak of the LDOS disappears, and so do the deep minima for $E < \Psi(B=0)$. In the dirty limit,

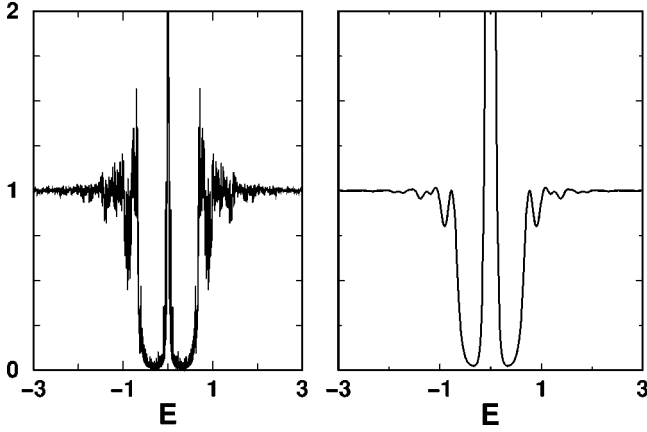


FIG. 3. (a) The LDOS $N(E, r=0)/N_0$ at the vortex center as a function of excitation energy E (in units πT_c). (b) $\sigma(E)/\sigma_N$ at the vortex center at $T=0.1T_c$. The two graphs are calculated for the clean limit.

$\xi/\ell \rightarrow \infty$, $N(r=0, E) = N_0$ for all quasiparticle energies.^{12,13}

A weak energy dependence of the LDOS at the vortex center was observed in dirty alloys $\text{Nb}_x\text{Ta}_{1-x}\text{Se}_2$ (see Ref. 5), a behavior expected for disordered superconductors. Also, a similar energy dependence of LDOS at the vortex center was measured in $\text{YNi}_2\text{B}_2\text{C}$.²⁷ It is now well established that nonmagnetic borocarbide superconductors ($\text{LuNi}_2\text{B}_2\text{C}$ and $\text{YNi}_2\text{B}_2\text{C}$) have nodes in the superconducting gap. Impurities smear out the gap anisotropy and anisotropic borocarbide superconductors with disorder can be considered as dirty s -wave materials. It was also found that the DOS measured at the vortex center in $\text{YNi}_2\text{B}_2\text{C}$ has a weak energy dependence, similar to the local density of states shown in Fig. 5 for dirty materials. From the residual resistivity ratio, the electron mean-free path in the sample used in Ref. 27 is estimated to be about 4 nm. This is shorter than the coherence length as estimated from the upper critical field. How-

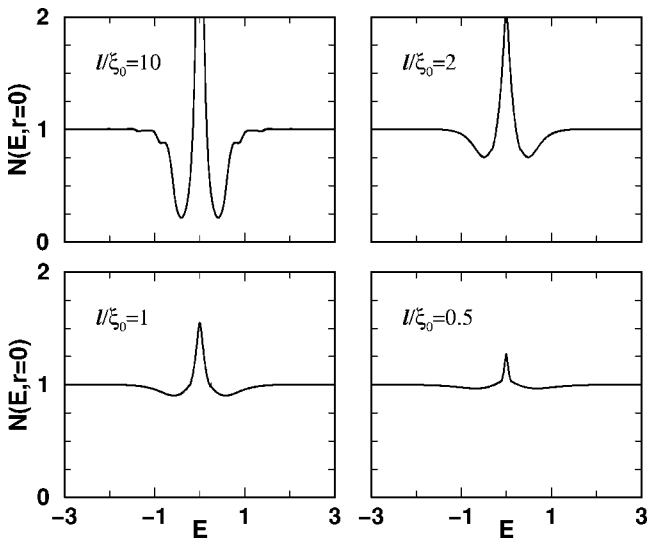


FIG. 4. The LDOS at the vortex center as a function of energy E plotted for four values of the mean-free path ℓ . σ/σ_N is almost indistinguishable from $N(E, r=0)/N_0$ at $T=0.1T_c$.

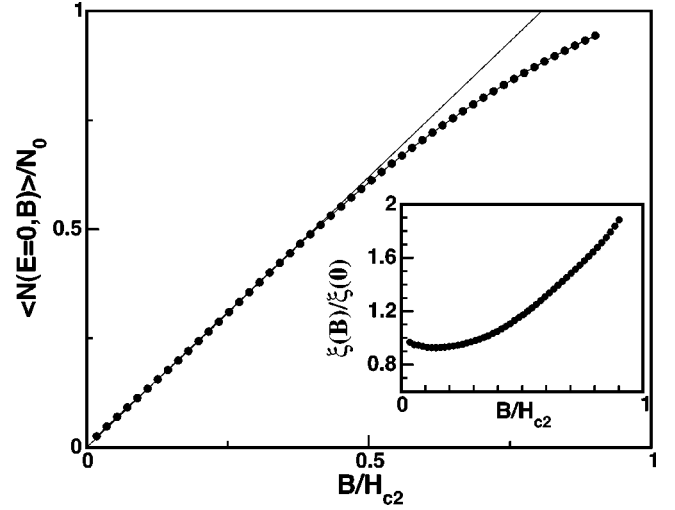


FIG. 5. The field dependence of spatially averaged zero-energy LDOS in the clean limit. The straight line is a guide for the eye. The inset: the normalized core size $\xi(B)/\xi(0)$ as a function of B/H_{c2} .

ever, BCS coherence length $\xi_0 = \hbar v_F / \pi \Delta_0$ is estimated to be much larger $\xi_0 \approx 30$ nm. Thus, superconducting sample $\text{YNi}_2\text{B}_2\text{C}$ studied by Sakata *et al.* can be considered to be in the dirty limit due to a small ratio $\ell/\xi_0 = 0.133$. The absence of a clear peak of DOS at zero energy near the vortex center, as well as the weak energy dependence of the density of states, is a consequence of a strong disorder in studied samples.

IV. LOCAL DENSITY OF STATES AND SPECIFIC HEAT

The low-energy quasiparticle excitations play an important role in the low-temperature thermodynamics. The specific heat $C_s(T)$ of a superconductor is given by

$$\frac{C_s}{T} = 2 \int_{-\infty}^{\infty} dE \frac{\partial \overline{N(E)}}{\partial T} \left\{ \ln \left[2 \cosh \left(\frac{E}{2T} \right) \right] - \frac{E}{2T} \tanh \frac{E}{2T} \right\} + 2 \int_{-\infty}^{\infty} \frac{E^2}{4T^3} \frac{\overline{N(E)} dE}{\cosh^2(E/2T)}. \quad (22)$$

One can utilize this expression only if the spatially averaged LDOS $\overline{N(E)}$ is provided. However, in the limit $T \rightarrow 0$, the first integral is zero. For small T , the integrand in the second integral is nonzero only in the small vicinity of $E=0$. Therefore, we can replace $\overline{N(E)}$ with $\overline{N(E=0)}$:

$$\gamma_s = \lim_{T \rightarrow 0} \frac{C_s}{T} = 2 \int_{-\infty}^{\infty} \frac{E^2}{4T^3} \frac{\overline{N(E=0)} dE}{\cosh^2(E/2T)} = \frac{2\pi^2 \overline{N(E=0)}}{3}. \quad (23)$$

In the normal phase, $C_n/T = 2\pi^2 N_0/3$, and we obtain the well-known result

$$\lim_{T \rightarrow 0} \frac{C_s}{C_n} = \frac{\overline{N(E=0)}}{N_0}. \quad (24)$$

If the low-energy quasiparticles are localized in the vortex cores, which is true for s -wave superconductors at least in

small fields, then $\overline{N(E=0)} \propto \xi^2/S_{\text{cell}}$. Here $S_{\text{cell}} = \Phi_0/B$ is the lattice cell area and ξ is the size of the vortex core. If we further assume that $\xi^2 \propto \Phi_0/H_{c2}$, then we arrive at the following scaling relationship $\overline{N(E=0)} \propto B/H_{c2}$, for s -wave superconductors. However, there are a number of reports on the nonlinear field dependence of $\gamma_s(H)$ in s -wave superconductors. One of the offered explanations is that the vortex core size ξ itself is field dependent which, in turn, leads to the nonlinear field dependence of the zero-energy DOS. The shrinking of the vortex core with increasing field is detected in NbSe₂ (Ref. 29) and YBa₂Cu₃O_{6.60}.³⁰ This is further supported by numerical calculations in the dirty^{13,29} and clean⁸ limits. Such an explanation brings out another puzzle. An experimental study on the influence of nonmagnetic impurities on the $\gamma_s(H)$ in Y(Ni_{1-x}Pt_x)₂B₂C and Nb_{1-x}Ta_xSe₂ revealed that linear $\gamma_s(H)$ is achieved only in dirty samples.³ This result suggests that the vortex core size in the dirty superconductors is field independent. However, numerical calculations by Golubov and Hartman,¹³ and by Sonnier *et al.*²⁹ show, that even in the dirty limit, ξ should shrink with increasing field.

Here we emphasize the necessity to evaluate the zero-energy DOS $N(0, \mathbf{r})$ at low temperatures in order to analyze the specific-heat data. In Ref. 8, a calculation for $T=0.5T_c$ revealed that $\overline{N(E=0)} \propto \xi^2(B)B$, where the vortex core radius $\xi(B)$ is independently calculated from the pair potential profile. At lower temperatures, Kramer and Pesch^{32,33} predict that the core radius shrinks and it might have a different field dependence compared to higher temperatures, as shown here.

The field dependence of $N(0, \mathbf{r})$ in the clean limit for $T=0.1T_c$ is shown in Fig. 5. In the inset we plot the field dependence of the core radius at the same temperature. Compared to the previously reported result at $T=0.5T_c$, where $\xi(B)$ decreases with field,⁸ the vortex core radius at $T=0.1T_c$ is nearly constant at low fields. As a consequence, the zero-energy $N(0, \mathbf{r})$ is a linear function of the magnetic induction.

In the clean limit the quantity $N(0, \mathbf{r})$ between vortices and far from the cores is negligible in fields as large as $B=0.4H_{c2}$. In other words, the main contributions to $N(0, \mathbf{r})$ is coming from the vortex cores. On the other hand, in the dirty limit, $N(0, \mathbf{r})$ is not confined to the vortex cores, but it is spread throughout the vortex lattice cell. It is large even in between vortices. Thus, the scaling relation $\overline{N(E=0)} \propto \xi^2(B)B$ is of no use in the dirty limit. This is the reason why we do not attempt to correlate the core size $\xi(B)$ and field dependence of LDOS in the impure case. However, $\overline{N(E=0, B)}$ is a linear function of magnetic induction at low fields for any impurity concentration: $\overline{N(E=0, B)}/N_0 = \alpha(\tau)B/H_{c2}$. Numerical results for $\overline{N(E=0, B)}/N_0$ as a function of ℓ are presented in Fig. 6. The constant of proportionality $\alpha(\tau)$ depends weakly on the electron mean-free path and saturates to $\alpha \approx 0.8$ in the dirty limit. The constant of proportionality goes from a value >1 (convex) in the clean case, to a value <1 (concave) in the dirty case. These results are similar to the analysis by Kita done near H_{c2} .³¹

Figure 7 shows the field dependence of the core radius ξ as calculated from pair potential profiles $\Psi(\mathbf{r})$. For a fixed

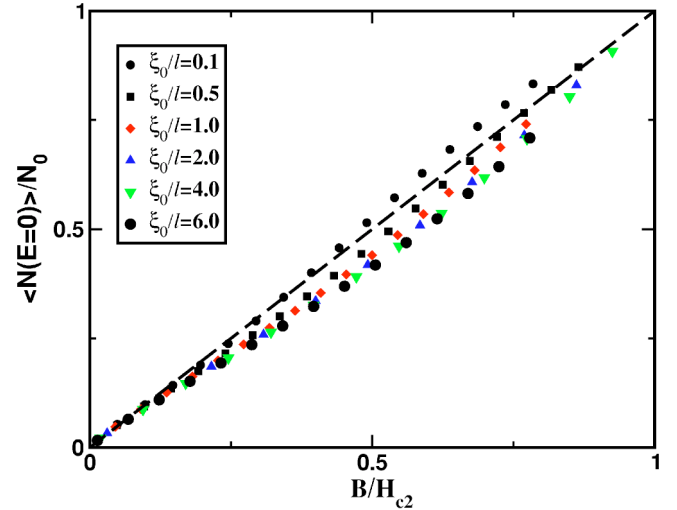


FIG. 6. The field dependence of the spatially averaged zero-energy LDOS for a few mean-free path ℓ .

reduced field B/H_{c2} , the radius is a nonmonotonic function of ξ_0/ℓ ; starting with the clean case, it increases sharply and then slowly decreases with increasing scattering. In the dirty limit, the core shrinks with increasing field, which is consistent with the previous calculations,^{13,29} in sharp contrast with the vortex core enlargement with increasing field in the clean limit. A small core size at low fields and temperatures is in accord with Kramer and Pesch.^{32,33} The core radius is calculated to be proportional to the temperature for a single vortex in the clean limit. Since the core radius has to become as large as the order of the coherence length near H_{c2} , it is reasonable that the core radius increases with increasing field at low temperatures. Our results also suggest that the Kramer-Pesch result does not work in the dirty case.

The experimental data, however, revealed that $\alpha=1$ in the dirty limit.³ This experimental data also shows the scaling $\overline{N(E=0, B)}/N_0 = \alpha(\tau)B/H_{c2}$ for all field values, a remarkable feature still to be explained. It is worth mentioning that in

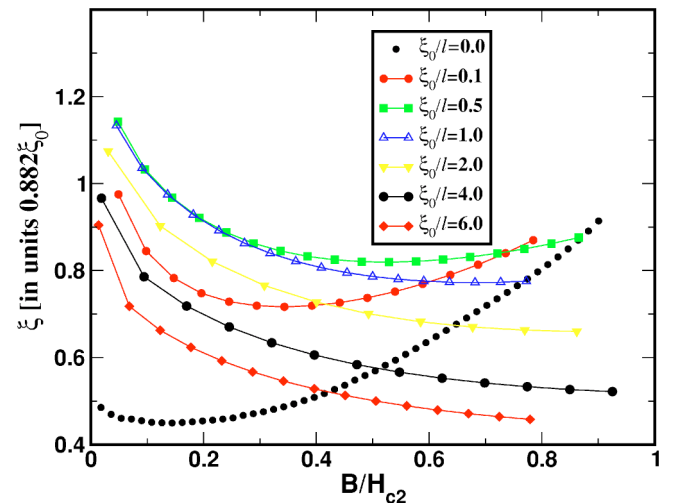


FIG. 7. Field dependence of the vortex core size for a few mean-free path.

Ref. 4, $C(B)$ is nonlinear in $Y(Ni_{1-x}Pt_x)_2B_2C$ for all $0 < x < 1$. In these materials, we need to take into account the gap anisotropy.

V. SUMMARY

In this paper we examined effect of nonmagnetic scattering on LDOS in the vortex lattice state in isotropic s -wave superconductors, by systematically changing the impurity concentration. We showed that the purity of the superconducting sample is crucial in forming the spatial structure of LDOS. As soon as impurities are introduced into the super-

conductor, scattered electrons lose the information on their initial state, and the sharp features of LDOS are flattened. We have calculated how the differential conductivity spectra evolve with the electron mean-free path. Although the impurities have a great impact on the LDOS, the spatially averaged LDOS shows a weak dependence on the reduced field B/H_{c2} .

ACKNOWLEDGMENTS

We acknowledge the useful communication with T. Dahm at the initial stage of this work. Also, we would like to thank V. G. Kogan for critically reading the text.

-
- ¹H. F. Hess, R. B. Robinson, R. C. Dynes, J. M. Valles, Jr., and J. V. Waszczak, *Phys. Rev. Lett.* **62**, 214 (1989).
²H. F. Hess, R. B. Robinson, and J. V. Waszczak, *Phys. Rev. Lett.* **64**, 2711 (1990).
³M. Nohara, M. Isshiki, F. Sakai, and H. Takagi, *J. Phys. Soc. Jpn.* **68**, 1078 (1999).
⁴D. Lipp, M. Schneider, A. Gladun, S.-L. Drechsler, J. Freudenberger, G. Fuchs, K. Nenkov, K.-H. Mülcer, T. Cichorek, and P. Gegenwart, *Europhys. Lett.* **58**, 435 (2002).
⁵Ch. Renner, A. D. Kent, Ph. Niedermann, and Ø. Fischer, *Phys. Rev. Lett.* **67**, 1650 (1991).
⁶S. Ullah, A. T. Dorsey, and L. J. Buchholtz, *Phys. Rev. B* **42**, 9950 (1990).
⁷U. Klein, *Phys. Rev. B* **41**, 4819 (1990).
⁸M. Ichioka, N. Hayashi, and K. Machida, *Phys. Rev. B* **55**, 6565 (1997).
⁹M. Eschrig, Ph.D thesis, University of Bayreuth (1997); cond-mat/9804330.
¹⁰Y. Kato and N. Hayashi, *J. Phys. Soc. Jpn.* **71**, 1721 (2002).
¹¹S. Dukan and Z. Tešanović, *Phys. Rev. B* **56**, 838 (1997).
¹²R. Watts-Tobin, L. Kramer, and W. Pesch, *J. Low Temp. Phys.* **17**, 71 (1974).
¹³A. A. Golubov and U. Hartmann, *Phys. Rev. Lett.* **72**, 3602 (1994).
¹⁴P. Miranović and K. Machida, *Phys. Rev. B* **67**, 092506 (2003).
¹⁵U. Klein, *J. Low Temp. Phys.* **69**, 1 (1987).
¹⁶E. V. Thuneberg, J. Kurkijärvri, and D. Rainer, *Phys. Rev. B* **29**, 3913 (1984).
¹⁷The numerical solution of Bogoliubov-de Gennes equations revealed little difference between LDOS in the two-dimensional and the three-dimensional case, see J. D. Shore, M. Huang, A. T. Dorsey, and J. P. Sethna, *Phys. Rev. Lett.* **62**, 3089 (1989).
¹⁸N. Schopohl, cond-mat/9804064.
¹⁹N. Schopohl and K. Maki, *Phys. Rev. B* **52**, 490 (1995).
²⁰U. Klein, *Phys. Rev. B* **41**, 4819 (1990).
²¹T. Dahm, S. Graser, C. Iniotakis, and N. Schopohl, *Phys. Rev. B* **66**, 144515 (2002).
²²D. Rainer, J. A. Sauls, and D. Waxman, *Phys. Rev. B* **54**, 10 094 (1996).
²³N. Hayashi, M. Ichioka, and K. Machida, *Phys. Rev. B* **56**, 9052 (1997).
²⁴B. Pöttinger and U. Klein, *Phys. Rev. Lett.* **70**, 2806 (1993).
²⁵P. G. de Gennes and D. Saint-James, *Phys. Lett.* **4**, 151 (1963).
²⁶W. J. Tomasz, *Phys. Rev. Lett.* **15**, 672 (1965).
²⁷H. Sakata, M. Oosawa, K. Matsuba, N. Nishida, H. Takeya, and K. Hirata, *Phys. Rev. Lett.* **84**, 1583 (2000).
²⁸J. M. Rowell and W. L. McMillan, *Phys. Rev. Lett.* **16**, 453 (1966).
²⁹J. E. Sonier, R. F. Kiefl, J. H. Brewer, J. Chakhalian, S. R. Dunsiger, W. A. MacFarlane, R. I. Miller, A. Wong, G. M. Luke, and J. W. Brill, *Phys. Rev. Lett.* **79**, 1742 (1997).
³⁰J. E. Sonier, J. H. Brewer, R. F. Kiefl, D. A. Bonn, S. R. Dunsiger, W. N. Hardy, R. Liang, W. A. MacFarlane, R. I. Miller, T. M. Riseman, D. R. Noakes, C. E. Stronach, and M. F. White, Jr., *Phys. Rev. Lett.* **79**, 2875 (1997).
³¹T. Kita (private communication).
³²L. Kramer and W. Pesch, *Z. Phys.* **269**, 59 (1974).
³³W. Pesch and L. Kramer, *J. Low Temp. Phys.* **15**, 367 (1974).